Supplementary Information

CNT Encapsulated MnO_x for Enhanced Flow-Through Electro-Fenton: The Involvement of Mn(IV)

Dongli Guo[a], Shengtao Jiang[b], Limin Jin[a], Kui Huang[c*], Ping Lu[d], Yanbiao Liu [a, e*]

[a] *Textile Pollution Controlling Engineering Center of Ministry of Environmental Protection, College of Environmental Science and Engineering, Donghua University, Shanghai 201620, China. E-mail: yanbiaoliu@dhu.edu.cn, Tel: +86 21 67798752.*

[b] *College of Life Science, Taizhou University, Taizhou 318000, China.*

[c] *School of Resources, Environment and Materials, Guangxi University, 100 Daxue Road, Nanning 530004, China. E-mail: khuang@gxu.edu.cn.*

[d] *Research Center for Analysis and Measurement, Donghua University, Shanghai 201620, China.*

[e] *Shanghai Institute of Pollution Control and Ecological Security, 1239 Siping Road, Shanghai 200092, China.*

Supplementary Information: 5 Texts, 5 Tables, and 22 Figures

Table of Contents

Text S1 Reagents and materials

Bisphenol A (BPA, >99.8%), sulfamethoxazole (SMX, 98.0%), 2,4,6-trichlorophenol (2,4,6-TCP, 98.0%), 4-chlorophenol (4-CP, ≥99%), phenol (99%), aniline (≥99%), methylene blue (MB, ≥97.0%), rhodamine B (RhB, ≥99%), benzoic acid (BA, 99.5%), 2,2,6,6-tetramethylpiperidine (TEMP, ≥98.0%), 5,5-dimethyl-1-pyrrolidine-N-oxide (DMPO, 97.0%), pyrophosphate (PP, 99.0%), and methyl phenyl sulfoxide (PMSO, >98.0%) were obtained from Shanghai Aladdin Biological Technology Co., Ltd. (China). $Mn(NO_3)_2$ (50%, w/w aq.) was purchased from Alfa Aesar Chemical Reagent Co., Ltd. (China). Nitric acid (HNO_3, 65.0~68.0%), sodium hydroxide (NaOH, ≥96.0%), sodium silicate ($Na_2SiO_3 \cdot 9H_2O$, ≥98.0%), sodium chloride (NaCl, ≥98.0%), sodium sulfate (Na_2SO_4, ≥99.0%), sodium nitrate ($NaNO_3$, ≥98.5%), levofloxacin (LFX), furfuryl alcohol (FFA, ≥98.5%), *tert*-butyl alcohol (TBA, ≥98.0%), *p*-benzoquinone (*p*-BQ, ≥98.0%), tetracycline (TC, ≥98.0%), and ethanol (≥96.0%) were purchased from Sinopharm Chemical Reagent Co. Ltd. (China). Methanol (≥99.9%), phosphoric acid, formic acid and acetonitrile (≥99.9%, chromatographic grade) were purchased from Titan Scientific Co., Ltd. (China). Multiwalled carbon nanotubes (CNTs) (<d> = 10-20 nm and <l> = 0.5-2.0 μm) were supplied by Nanjing XFNANO Materials Tech Co., Ltd. (China). All chemical reagents were used without any purification. Lake water, pharmaceutical wastewater and waste water treatment plant secondary effluent was collected from the Jingyue Lake of Donghua university campus, a hospital, and a waste water treatment plant of Shanghai, respectively. The wastewater characteristics were available in Table S1. Ultrapure water (resistivity ≥18.2 MΩ cm) was used in all experiments.

Text S2 Preparation of MnO_x-in-CNT and MnO_x-out-CNT filters

The MnO_x nanoparticles were introduced into the CNT channels by a wet-chemistry method.[1] The detailed prepared processes are described as follows. Raw CNTs (<d> = 10-20 nm and <l> = 0.5-2.0 μm, purchased from Xianfeng Nano Co. Ltd.) were first opened up by refluxing in HNO_3 (65~68 wt. %) at 140 ºC for 14 h. The metal catalyst residues were removed during this process. The resulting CNT were immersed into an aqueous $Mn(NO_3)_2$ solution, which was introduced into the CNT channels

utilizing the capillary forces of CNT aided by ultrasonic treatment and stirring. After the resulting slurry mixture was dried at room temperature, it was gradually heated to 210ºC and held for 1 h. By this process, $Mn(NO_3)_2$ decomposes into MnO_x and the obtained sample is denoted as MnO_x-in-CNT.

For comparison, the same loadings of MnO_x were deposited on the outer surface of carbon nanotubes by impregnating CNT with aqueous $Mn(NO_3)_2$ solution. These CNT with closed caps were obtained by refluxing raw CNT in 37 wt. % HNO_3 solution at 110ºC for 5 h. Then, MnO_x-out-CNT was obtained after the same drying procedure.

The hybrid filters and pristine CNT filter can be fabricated by a facile vacuum filtration route. Briefly, 30 mg of MnO_x-out-CNT, MnO_x-in-CNT or CNT powders were dispersed into 40 mL N-mmethyl-2-pyrrolidinone (NMP) and probe-sonicating for 40 min (100 W, LABSONIC® M, Sartorius) to achieve a homogeneous suspension solution. The mixture was then vacuum-filtered onto a polytetrafluoroethylene (PTFE) membrane and washed sequentially with 100 mL of ethanol and 200 mL of DI-H_2O before use.

Text S3 Calculation of H_2O_2 flux

The H_2O_2 flux was evaluated in the absence of BPA, and the result was calculated by the following equation:[2]

$$H_2O_2 \text{ Flux} = \frac{(H_2O_2)(\text{mmol/L}) \times \text{flow rate(L/h)}}{\text{effective filter area } (m^2)} \quad (1)$$

where an *Effective filter area* represents the area that is permeable to a solution *i.e.*, 7.1×10^{-4} m^2.

Text S4 Computational methods

A CNT model with C-C bond length of 1.42 Å was constructed. The MnO_x cluster was constructed, and the structure was taken from Mn_5O_8, as it encompasses both trivalent and tetravalent Mn. The MnO_x was placed inside and outside the CNT, respectively, thus constituting the confined and unconfined model with a cell size of 19.62 × 17.22 × 36.27 and α, β, γ all at 90°. CP2K 8.1[3] was used for the geometric optimization of the configuration and single-point energy calculations. The theoretical method was PBE[4] and the basis group was DZVP-MOLOPT-SR-GTH.[5] The OT

acceleration algorithm, DFT-D3 (BJ)[5,6] correction was used. In addition, Broyden mixing as density matrix mixing method were applied. Since the system already has more than 15 Å in the XYZ direction, only one Γ point was needed. The SCF convergence limit is set as 5×10^{-6}, and the cutoff and REL cutoff were set as 400 and 55 Ry, respectively. The binding energy is calculated according to the following formula:

$$E = (E_{product} - \sum n_i * E_{atom\_i})/n \quad (2)$$

where E is the binding energy, $E_{product}$ is the energy of the product, which refers to the energy of the CNT binding the corresponding configurations such as H_2O_2, Mn(IV), $HO^{\bullet}$, $O_2^{\bullet-}$, *etc.*, E_{atom_i} is the energy of the atom i that constitutes the product, n_i is the number of i atoms, and n is the total number of atoms in the product.

The ab initio calculations were conducted using the Gaussian 09 package.[7] The geometry optimization and frequency calculation for the BPA molecule were carried out at the B3LYP/6-311G* level. The Fukui functions representing the electrophilic (f^-) were applied to unveil the active sites of the BPA molecule by Multiwfn.[8]

Text S5 Calculation of energy consumption

The energy consumption was calculated in terms of per volume treated water (kW h/m^3) or the removal of per gram BPA from the simulated wastewater sample (kW h/g):[9]

$$energy\ consumption\ (\mathrm{kW\ h\ m^{-3}}) = \frac{1000UIt}{V_0} \quad (3)$$

$$\text{energy consumption (kW h g}^{-1}\text{ BPA)} = \frac{UIt}{(C_0 - C_t)V_0} \quad (4)$$

where *U* is the applied voltage (V), *I* is the applied current (A), *t* represents the treatment time (h), V_0 denotes the solution volume (L), C_0 and C_t are the BPA concentration in the solution (mg L^{-1}) at time *0* and *t*, respectively. Here, the electric energy consumption is converted accordingly to U.S. environmental prices (US$) and the average electricity price is 14.31 cents per kWh (June, 2022).

Table S1 HPLC operation parameters for different substrates.

Substrates	Methanol	Acetonitrile	DI (0.1% phosphoric acid)	DI	Detection wavelength (nm)	Flow rate (mL min^{-1})
BPA	70	-	-	30	230	1.0
SMX	30	-	70	-	300	1.0
4-CP		40		60	210	1.0
2,4,6-TCP	-	70	30	-	294	1.0
TC		70	30		280	0.5
LFX	-	85	15	-	293	1.0
phenol	60	-	40	-	270	1.0
aniline	40	-		60	230	0.5
BA		15		85	270	0.5
PMSO		20		80	230	0.8
$PMSO_2$		20		80	215	0.8

Table S2 Comparison of the BPA degradation efficiency in the proposed system with reported literature.

Materials	BPA concentration	Oxidant	Reaction time	pH	Removal efficiency	References
nFe_2O_3/MIL-53(Cu)	0.044 mM (10 mg L^{-1})	H_2O_2	120 min	5.0	77.2%	10
RGO-CeO_2-TNAs	0.044 mM (10 mg L^{-1})	H_2O_2	120 min	5.0	81.8%	11
AlgCMC-Fe	0.022 mM (5 mg L^{-1})	H_2O_2	240 min	7.0	87.0%	12
Co_3O_4 hollow nanospheres	0.175 mM (40 mg L^{-1})	persulfate	100 min	6.0	91.0%	13
Cu(0.05)-$AlPO_4$	0.11 mM (25 mg L^{-1})	H_2O_2	180 min	7.0	92.0%	14
Cu-Al_2O_3	0.088 mM (20 mg L^{-1})	H_2O_2	180 min	7.0	87.0%	15
$LaCu_{0.5}Fe_{0.5}O_{3-\delta}$	0.088 mM (20 mg L^{-1})	H_2O_2	120 min	6.0	92.1%	16
Fe_3O_4 supported on coal fly ash	0.22 mM (50 mg L^{-1})	persulfate	120 min	5.0	80.2%	17
goethite	0.1 mM (22.8 mg L^{-1})	H_2O_2	240 min	4.5	75.9%	18
Fe_2O_3-in-CNT	0.04 mM (9.1 mg L^{-1})	H_2O_2	180 min	6.8	85.7%	2
MnO_x-in-CNT	0.022 mM (5 mg L^{-1})	H_2O_2	120 min	6.5	93.3%	this study

Table S3 Comparison of the performance of the proposed system with reported Mn-based catalysts.

Materials	Pollutants	Oxidant	pH	Removal efficiency	References
Mn_3O_4	bisphenol-AF	persulfate	7.0	90.0%	19
Mn@porous carbon	triclosan	H_2O_2	3.0	83.3%	20
MnO_2/CNTs	phenol	H_2O_2	natural	90.0%	21
Cu/MnO	benzotriazo	H_2O_2	7.13	89.0%	22
MnO	ciprofloxacin	persulfate	5.0	84.3%	23
Mn_2O_3	ciprofloxacin	persulfate	5.0	56.2%	23
MnO_x-in-CNT	BPA	H_2O_2	6.5	93.3%	this study

Table S4 Quality parameters of different water used for BPA removal by MnO_x-in-CNT electro-Fenton system.

Samples	pH	DO (mg L^{-1})	TOC (mg L^{-1})	Conductivity (μs cm^{-1})
Tap water	7.1	9.2	1.6	513.4
Lake water	7.6	8.6	85.3	675.6
Secondary effluent	6.8	8.2	135.7	642.3
Pharmaceutical water	7.4	6.3	261.6	654.1

Table S5 Chemicals used as model organic pollutants.

Compounds	Structure	CAS No.	Formula	Industrial use	Health risk
BPA	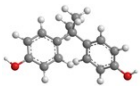	80-05-7	$C_{15}H_{16}O_2$	Producing plastics, polymers, and fine chemicals	Endocrine disruption
4-CP	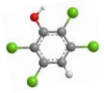	106-48-9	C_6H_5ClO	Agricultural chemicals/dyes/drugs manufacturing	Endocrine disruption and reproductive toxicity
2,4,6-TCP	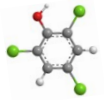	88-06-2	$C_6H_3Cl_3O$	Insecticide/fungicide/herbicide	Endocrine disruption and reproductive toxicity
Phenol		108-95-2	C_6H_6O	Resins/fungicides/preservatives/drugs manufacturing	Threats to aquatic ecosystems
SMX	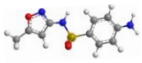	723-46-6	$C_{10}H_{11}N_3O_3S$	Antibiotic	Threats to aquatic ecosystems
TC	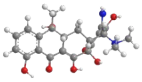	60-54-8	$C_{22}H_{24}N_2O_8$	Antibiotic	Damage to human health
LFX	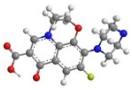	100986-85-4	$C_{18}H_{20}FN_3O_4$	Antibiotic	Threats to aquatic ecosystems
MB	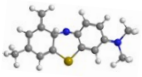	7220-79-3	$C_{16}H_{18}ClN_3S.3H_2O$	Dyes	Toxic, carcinogenic, or mutagenic to life forms
RhB	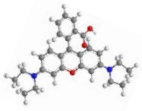	547-58-0	$C_{28}H_{31}C_lN_2O_3$	Dyes	Toxic, carcinogenic, or mutagenic to life forms
Aniline	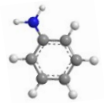	62-53-3	C_6H_7N	Dyes/pesticides/pharmaceutical compounds	Carcinogen
BA	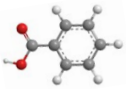	65-85-0	$C_7H_6O_2$	Cosmetic/drugs/food industries	Threats to ecosystem and human health

Note: The compound geometries were drawn using Chem3D software (ChemOffice Professional 19.0). Gray = carbon, red = oxygen, white = hydrogen, blue = nitrogen, and green = chloride.

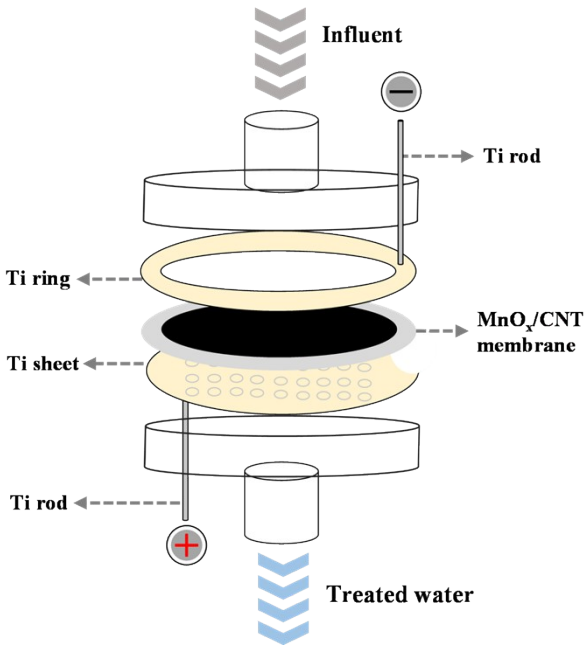

Fig. S1 Schematic representation of the flow-through electroactive filtration reactor.

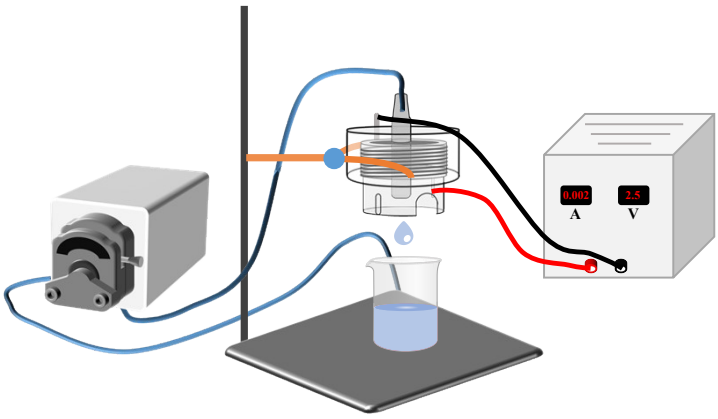

Fig. S2 Schematic illustration of the flow-through electro-Fenton system.

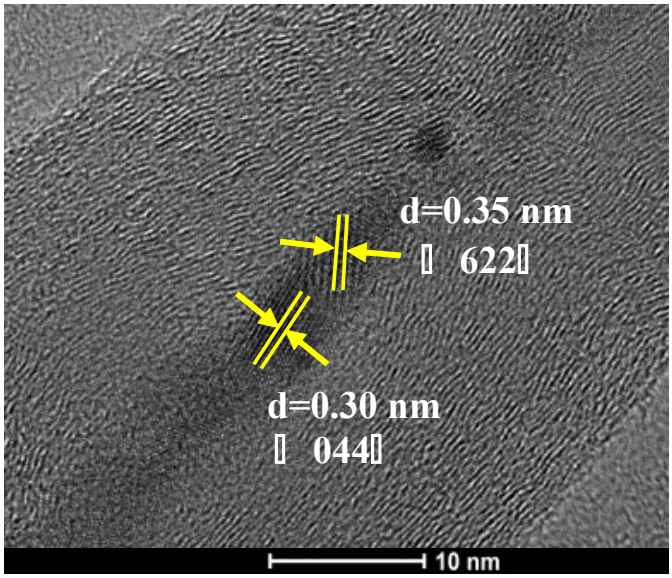

Fig. S3 HRTEM image of MnO_x-in-CNT filter.

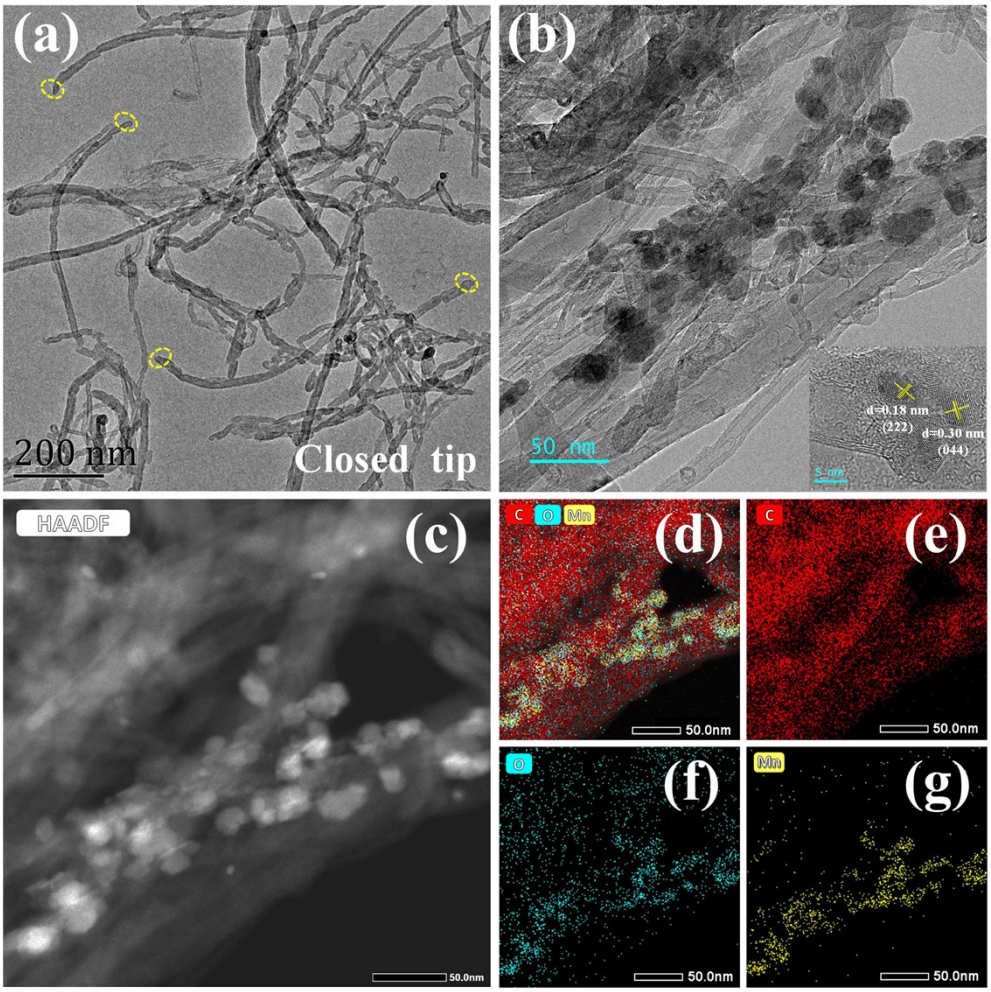

Fig. S4 (a) TEM image of CNT with closed tip; (b) TEM image of MnO_x-out-CNT filter (Inset) HRTEM image of MnO_x nanoparticles; (c) HAADF-STEM image of MnO_x-out-CNT filter; (d) EDS mapping pattern with C, O, and Mn elements overlapping together; EDS elemental mapping of (d) C, (e) O, and (f) Mn.

The HRTEM image (inset) illustrates two lattice stripe spacings of 0.18 and 0.30 nm, being in good agreement with the {222} and {044} crystal planes of Mn_2O_3, respectively.

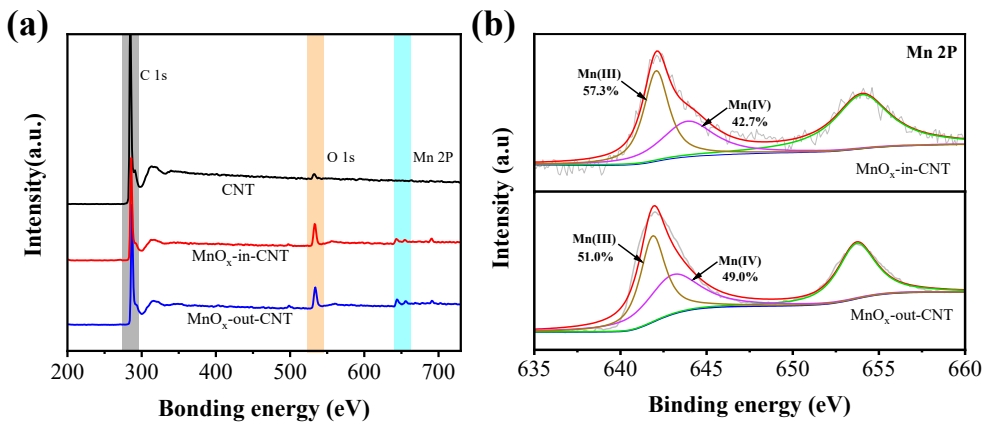

Fig. S5 (a) XPS wide scan survey spectra and (b) high-resolution Mn 2p spectra of different catalysts.

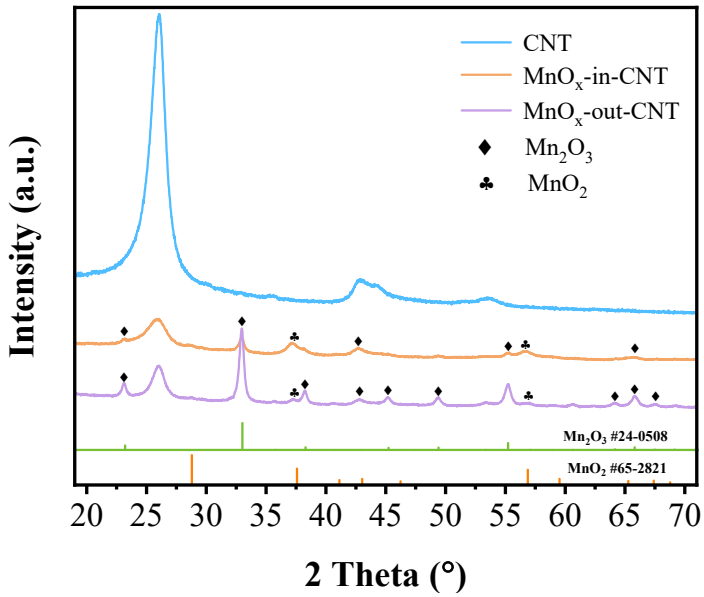

Fig. S6 XRD patterns of CNT, MnO_x-in-CNT, and MnO_x-out-CNT.

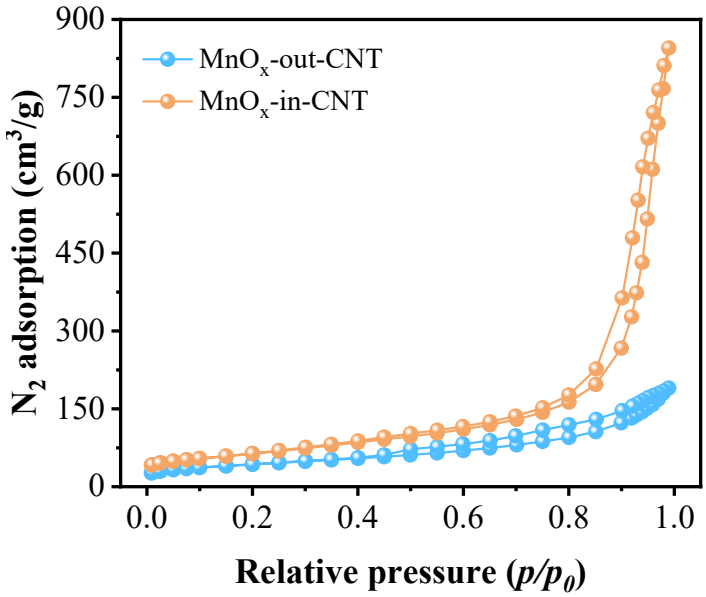

Fig. S7 N_2 adsorption–desorption isotherms of MnO_x-out-CNT and MnO_x-in-CNT.

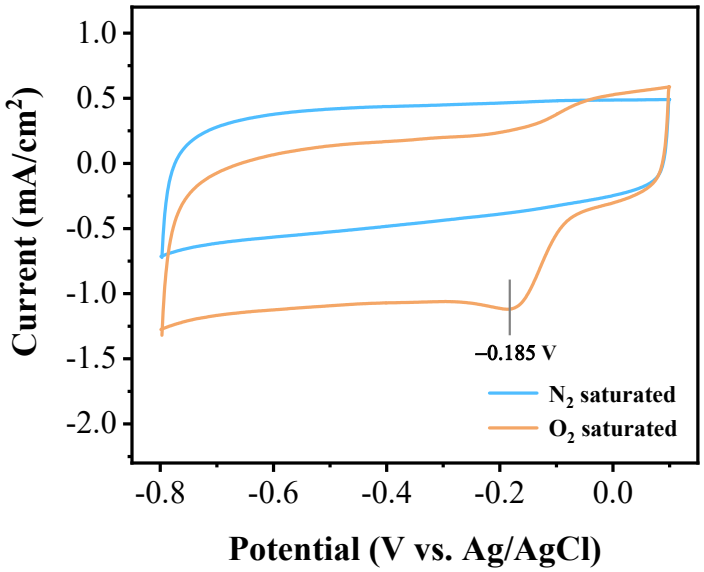

Fig. S8 CV curves of CNT filter in O_2- and N_2-saturated 50 mM Na_2SO_4 solution at pH 6.5 at a scan rate of 10 mV s^{-1}.

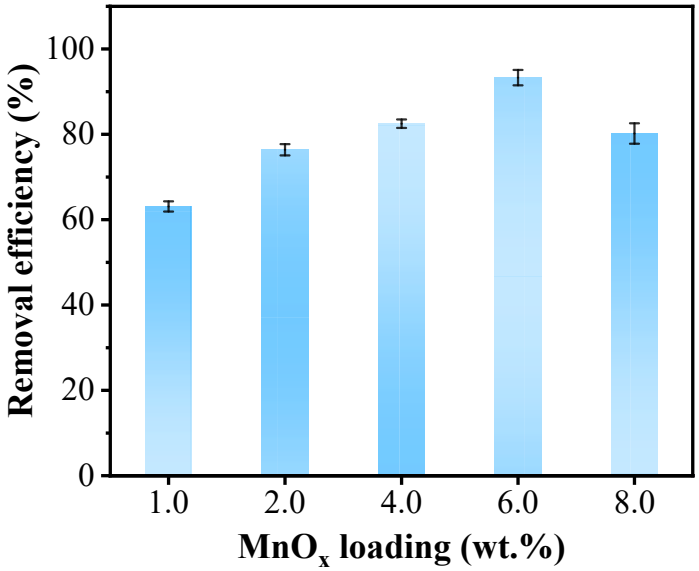

Fig. S9 Effect of MnO_x loading on BPA degradation. Experimental conditions: $[BPA]_0$ = 0.022 mM, $[pH]_0$ = 6.5, $[DO]_0$ = 38.3 ± 1.6 mg L^{-1}, flow rate = 1.5 mL min^{-1}, and $[Na_2SO_4]$ = 10 mM.

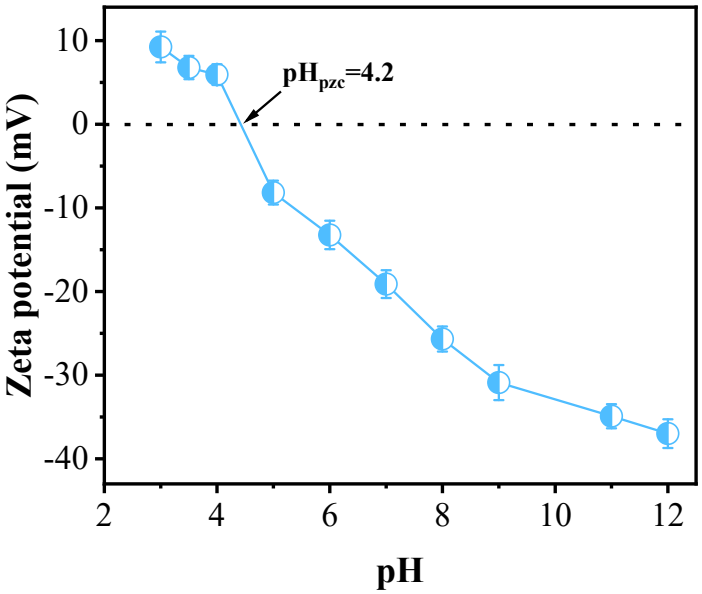

Fig. S10 Zeta potential of MnO_x versus solution pH.

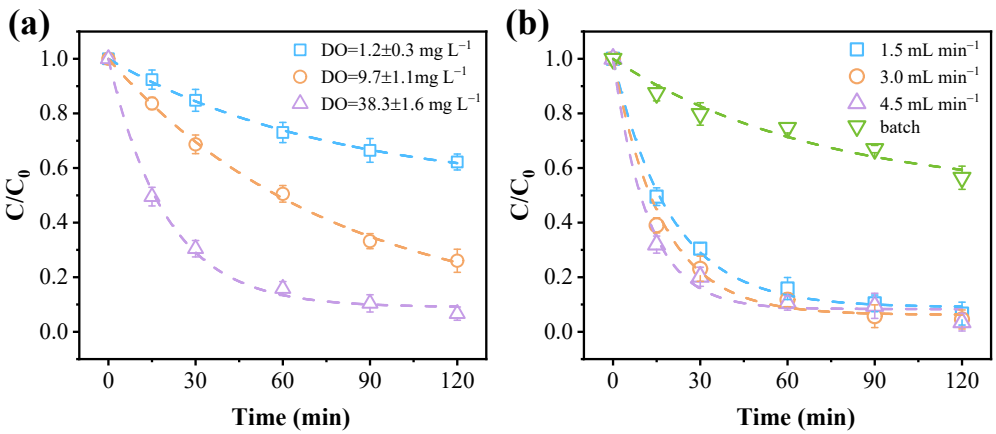

Fig. S11 Effect of (a) DO and (b) flow rate on BPA degradation. Experimental conditions: $[BPA]_0$ = 0.022 mM, $[pH]_0$ = 6.5, and $[Na_2SO_4]$ = 10 mM.

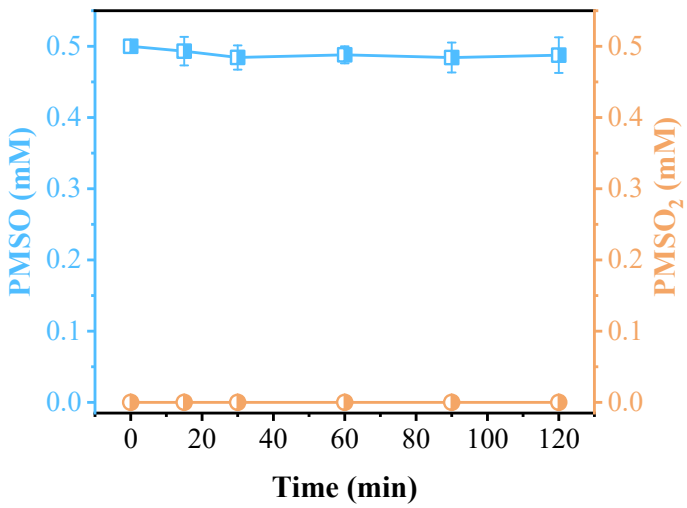

Fig. S12 Decline of PMSO and production of $PMSO_2$ in the MnOx-in-CNT electro-Fenton system. Experimental conditions: $[PMSO]_0$ = 0.5 mM, $[pH]_0$ = 6.5, $[DO]_0$ = 38.3 ± 1.6 mg L^{-1}, flow rate = 1.5 mL min^{-1}, and $[Na_2SO_4]$ = 10 mM.

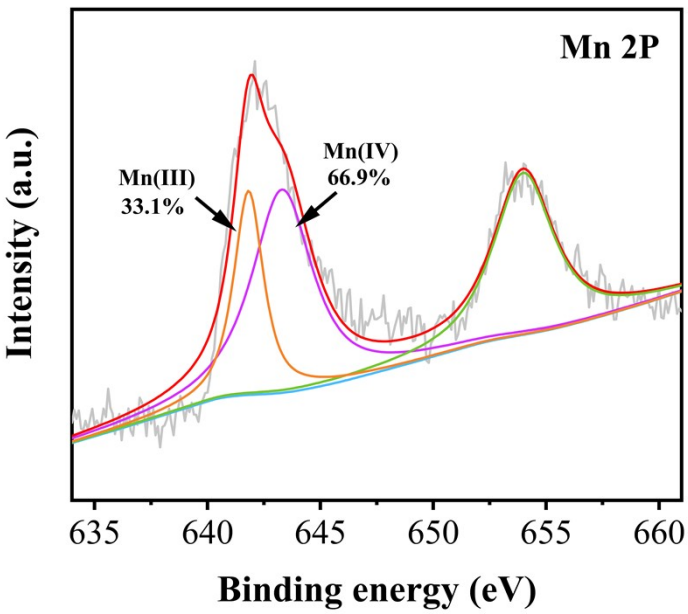

Fig. S13 XPS spectrogram and the fitting peak of Mn 2p of after used MnO_x-in-CNT filter.

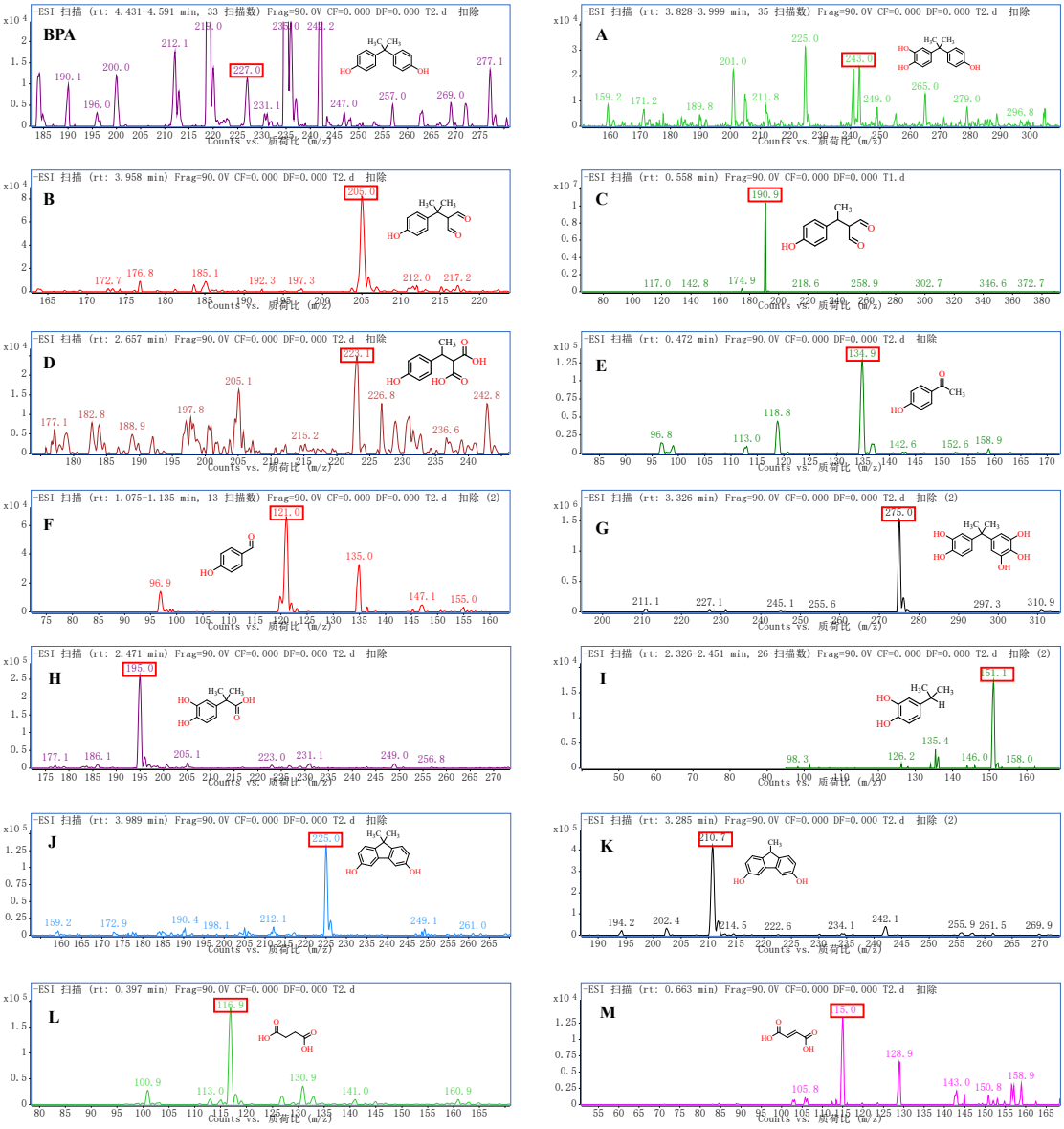

Fig. S14 Mass spectrum of BPA and intermediates during the BPA removal in MnO_x-in-CNT electro-Fenton system.

(a)

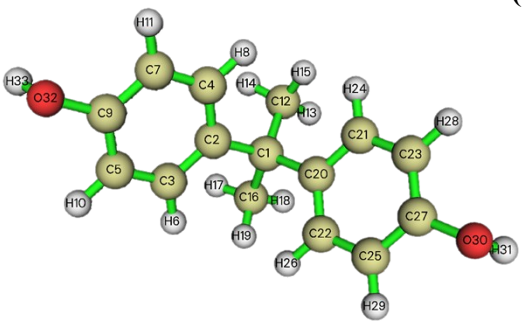

(b)

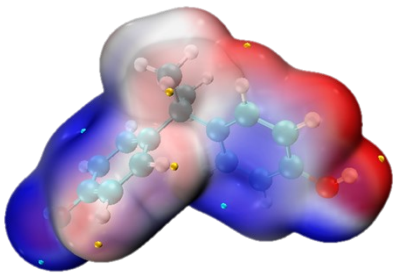

(c)

Atom	No	Charge(0) (e/a.u.)	Charge(+1) (e/a.u.)	Charge(-1) (e/a.u.)	f^-
C	1	-0.06424	-0.04762	-0.0244	0.0044
C	2	-0.05898	0.11295	-0.03287	0.0483
C	3	-0.19516	-0.07123	-0.07773	0.0337
C	4	-0.17956	-0.05841	-0.05615	0.0271
C	5	-0.28734	-0.10152	-0.10953	0.0513
H	6	0.20835	0.11426	0.09217	0.0219
C	7	-0.24682	-0.11887	-0.09806	0.0367
H	8	0.21384	0.11092	0.09234	0.0158
C	9	0.3389	0.28332	0.15212	0.054
H	10	0.20004	0.11236	0.08416	0.0292
H	11	0.21915	0.12206	0.09394	0.0255
C	12	-0.56789	-0.28519	-0.28198	0.0122
H	13	0.19652	0.10934	0.09422	0.0175
H	14	0.20762	0.1129	0.09574	0.0154
H	15	0.20319	0.10098	0.09747	0.0089
C	16	-0.5679	-0.2852	-0.28197	0.0122
H	17	0.19652	0.10934	0.09422	0.0175
H	18	0.20763	0.1129	0.09573	0.0154
H	19	0.20319	0.10098	0.09747	0.0089
C	20	-0.05899	0.11289	-0.03285	0.0483
C	21	-0.19516	-0.07124	-0.07789	0.0337
C	22	-0.17955	-0.05841	-0.05599	0.0271
C	23	-0.28736	-0.10153	-0.10951	0.0513
H	24	0.20835	0.11426	0.09218	0.0219
C	25	-0.24682	-0.11888	-0.09819	0.0367
H	26	0.21384	0.11092	0.09235	0.0158
C	27	0.33891	0.28328	0.15216	0.054
H	28	0.20005	0.11236	0.08417	0.0292
H	29	0.21915	0.12205	0.09395	0.0255
O	30	-0.67909	-0.26268	-0.35447	0.0731
H	31	0.45935	0.24268	0.22086	0.0274
O	32	-0.67908	-0.26265	-0.35448	0.0731
H	33	0.45934	0.24268	0.22086	0.0274

Fig. S15 (a) The geometrical structure of BPA, (b) electrostatic potential (ESP) map of BPA, and (c) natural population analysis (NPA) charge distribution and Fukui index of BPA.

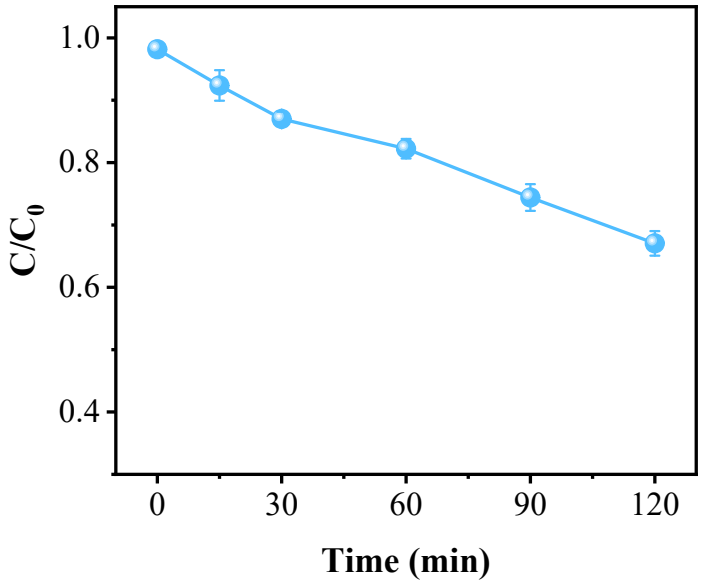

Fig. S16 TOC removal in the MnO_x-in-CNT electro-Fenton system. Experimental conditions: $[BPA]_0$ = 0.022 mM, $[pH]_0$ = 6.5, voltage = –2.5 V, $[DO]_0$ = 38.3 ± 1.6 mg L^{-1}, $[Na_2SO_4]$ = 10 mM, and flow rate = 1.5 mL min^{-1}.

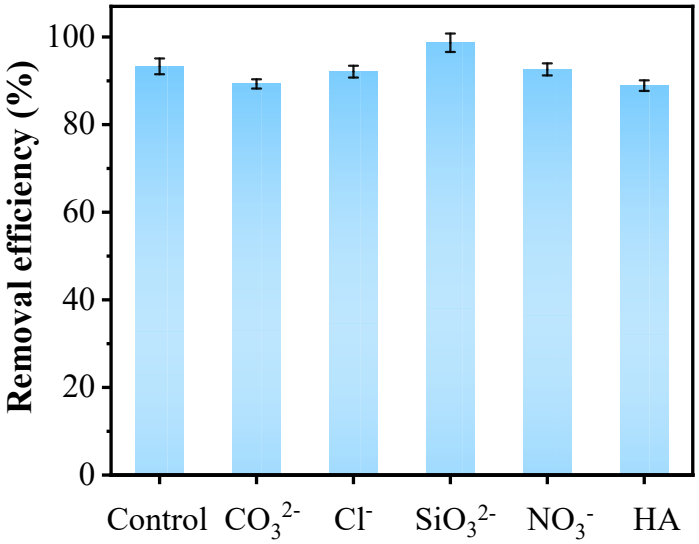

Fig. S17 Effect of co-existing substrates on the degradation of BPA by MnO_x-in-CNT electro-Fenton system. Experimental conditions: $[BPA]_0$ = 0.022 mM, $[pH]_0$ = 6.5, voltage = –2.5 V, [CO_3^{2-}, Cl^-, SiO_3^{2-}, NO_3^-] = 10.0 mM, and [HA] = 5.0 mg L^{-1}, $[DO]_0$ = 38.3 ± 1.6 mg L^{-1}, [Na_2SO_4] = 10 mM, and flow rate = 1.5 mL min^{-1}.

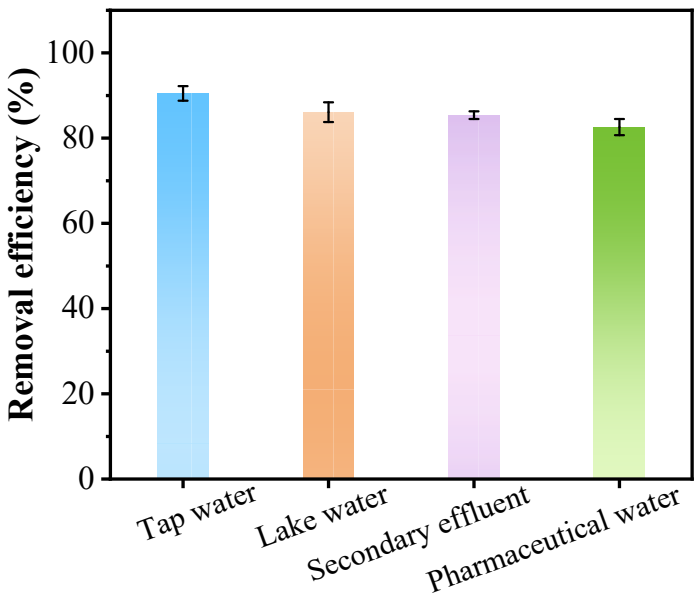

Fig. S18 Effect of different water matrices on the degradation of BPA by MnO_x-in-CNT electro-Fenton system. Experimental conditions: $[BPA]_0$ = 0.022 mM, $[pH]_0$ = 6.5, voltage = –2.5 V, $[DO]_0$ = 38.3 ± 1.6 mg L^{-1}, $[Na_2SO_4]$ = 10 mM, and flow rate = 1.5 mL min^{-1}.

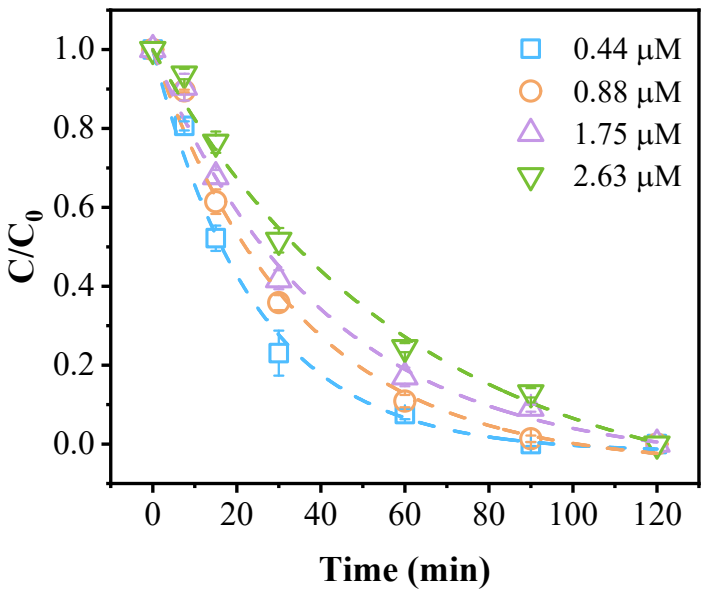

Fig. S19 The performance of trace BPA degradation in the MnO_x-in-CNT electro-Fenton system. Experimental conditions: $[pH]_0$ = 6.5, voltage = –2.5 V, $[DO]_0$ = 38.3 ± 1.6 mg L^{-1}, $[Na_2SO_4]$ = 10 mM, and flow rate = 1.5 mL min^{-1}.

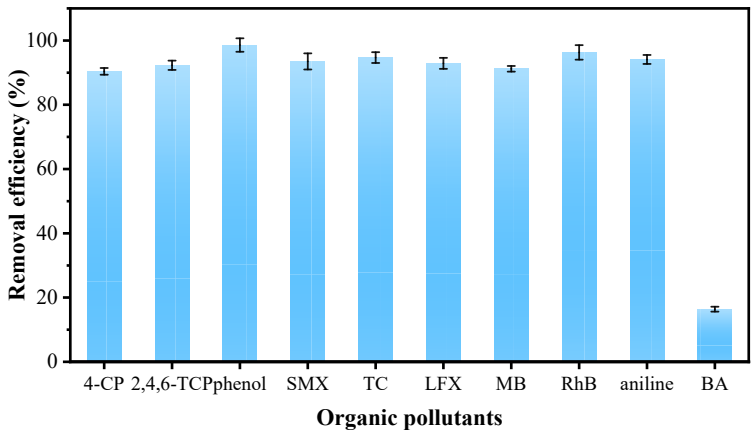

Fig. S20 Degradation of various organic pollutants in the MnO_x-in-CNT electro-Fenton system. Experimental conditions: $[4\text{-CP}]_0 = [2,4,6\text{-TCP}]_0 = [\text{phenol}]_0 = [\text{SMX}]_0 = [\text{LFX}]_0 = [\text{TC}]_0 = [\text{MB}]_0 = [\text{RhB}]_0 = [\text{aniline}]_0 = [\text{BA}]_0 = 0.022$ mM, $[\text{pH}]_0 = 6.5$, voltage = –2.5 V, $[\text{DO}]_0 = 38.3 \pm 1.6$ mg L^{-1}, $[Na_2SO_4] = 10$ mM, and flow rate = 1.5 mL min^{-1}.

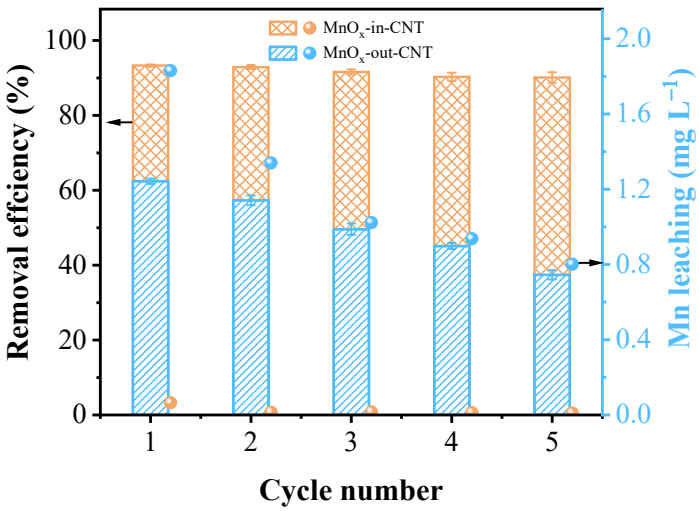

Fig. S21 A comparison of BPA degradation stability and leached total Mn concentration of the MnO_x-in-CNT or MnO_x-out-CNT electro-Fenton system. Experimental conditions: $[BPA]_0$ = 0.022 mM, $[pH]_0$ = 6.5, voltage = –2.5 V, $[DO]_0$ = 38.3 ± 1.6 mg L^{-1}, $[Na_2SO_4]$ = 10 mM, and flow rate = 1.5 mL min^{-1}.

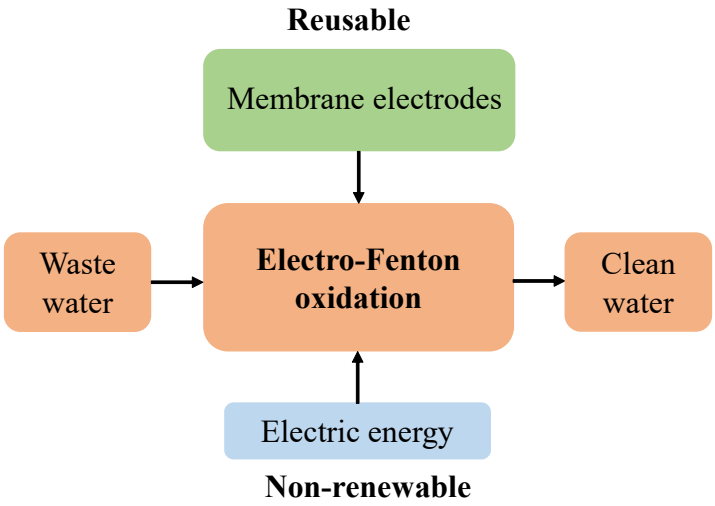

Fig. S22 Flow path of the MnO_x-in-CNT electro-Fenton system.

References

1 W. Chen, Z. Fan, L. Gu, X. Bao and C. Wang, *Chem. Commun.*, 2010, **46**, 3905-3907.

2 D. L. Guo, Y. B. Liu, H. D. Ji, C. C. Wang, B. Chen, C. S. Shen, F. Li, Y. X. Wang, P. Lu and W. Liu, *Environ. Sci. Technol.*, 2021, **55**, 4045-4053.

3 J. Hutter, M. Iannuzzi, F. Schiffmann and J. VandeVondele, *Wires Comput. Mol. Sci.*, 2014, **4**, 15-25.

4 M. Ernzerhof and G. E. Scuseria, *J Chem. Phys.*, 1999, **110**, 5029-5036.

5 S. E. Boulfelfel, P. I. Ravikovitch, L. Koziol and D. S. Sholl, *J. Phys. Chem. C*, 2016, **120**, 14140-14148.

6 S. Grimme, *J Comput. Chem.*, 2006, **27**, 1787-1799.

7 J. P. Perdew, A. Ruzsinszky, J. M. Tao, V. N. Staroverov, G. E. Scuseria and G. I. Csonka, *J Chem. Phys.*, 2005, **123**, 062201.

8 T. Lu and F. W. Chen, *J Comput. Chem.*, 2012, **33**, 580-592.

9 C. Flox, P. L. Cabot, F. Centellas, J. A. Garrido, R. M. Rodriguez, C. Arias and E. Brillas, *Appl. Catal., B*, 2007, **75**, 17-28.

10 Y. Ren, M. Q. Shi, W. M. Zhang, D. D. Dionysiou, J. H. Lu, C. Shan, Y. Y. Zhang, L. Lv and B. C. Pan, *Environ. Sci. Technol.*, 2020, **54**, 5258-5267.

11 Q. X. Zhou, A. Xing, J. Li, D. C. Zhao, K. F. Zhao and M. Lei, *Electrochim. Acta*, 2016, **209**, 379-388.

12 D. D. Bezerra, R. J. Franca and M. R. D. Marques, *Catal. Letters*, 2021, **151**, 1477-1487.

13 J. Hu, X. K. Zeng, G. Wang, B. B. Qian, Y. Liu, X. Y. Hu, B. He, L. Zhang and X. W. Zhang, *Chem. Eng. J.*, 2020, **400**, 125869.

14 L. L. Zhang, D. A. Xu, C. Hu and Y. L. Shi, *Appl. Catal., B*, 2017, **207**, 9-16.

15 Y. Wang, J. Li, J. Y. Sun, Y. B. Wang and X. Zhao, *J. Mater. Chem. A*, 2017, **5**, 19151-19158.

16 K. L. Pan, C. Z. Yang, J. P. Hu, W. L. Yang, B. C. Liu, J. K. Yang, S. Liang, K. K. Xiao and H. J. Hou, *J. Hazard. Mater.*, 2020, **389**, 122072.

17 X. M. Xu, S. Y. Zong, W. M. Chen and D. Liu, *Chem. Eng. J.*, 2019, **369**, 470-479.

18 J. F. Ding, L. L. Shen, R. P. Yan, S. H. Lu, Y. N. Zhang, X. F. Zhang and H. J. Zhang, *Chemosphere*, 2020, **261**, 127715.

19 N. R. Wang, J. Zhang, Y. L. Zhang, P. Zhou, J. Q. Wang and Y. Liu, *Chemosphere*, 2021, **263**, 127950.

20 X. L. Zhou, D. Xu, Y. C. Chen and Y. Y. Hu, *Chem. Eng. J.*, 2020, **384**, 123324.

21 C. Qu, Y. G. Li, S. J. Meng, X. H. Li, S. J. Zhang and D.-W. Liang, *J. Hazard. Mater.*, 2022, **434**, 128923.

22 Y. T. Zhang, C. Liu, B. B. Xu, F. Qi and W. Chu, *Appl. Catal., B*, 2016, **199**, 447-457.

23 Y. Chi, P. Wang, M. Lin, C. Lin, M. Gao, C. L. Zhao and X. Wu, *Chemosphere*, 2022, **299**, 134437.